CALCULATION ALGORITHMS AND THE NUMERICAL SIMULATION OF TRANSIENT WAVE PROCESSES IN ELASTIC SOLIDS AND STRUCTURES

S. Abdukadirov[a] and M. Ayzenberg-Stepanenko[b]

[a]Tashkent Architecture and Construction Institute, Tashkent, Uzbekistan
[b]Ben-Gurion University of the Negev, Beer-Sheva, Israel

Abstract. The transient processes in elastic solids and structures. Advanced numerical algorithms are developed intended for computer simulations of waves possessing front gaps and high-gradient components. The algorithms are constructed with the condition that dependence domains are maximally closed in differential and difference equations corresponding continual and discrete description of wave processes, respectively. The designed explicit calculation algorithms suppress the influence of spurious effects of numerical dispersion that allows discontinuities in fronts and high-gradient components to be accurately computed. A set of examples of computer simulations of linear and nonlinear wave processes are presented. Among them are (a) longitudinal impact to a rod upon elastic foundation, (b) cylindrical and spherical waves in a compressible liquid, (c) dynamics of periodical structural systems, and (d) wave propagation in a unidirectional composite shield.

1 INTRODUCTION

Exact calculation of the wave fronts and strongly varying perturbations always of utmost importance for problems of numerical simulation of wave/fracture processes in solid and, especially, in composite structures.

Significant rise in influence of the composite microstructure on the wave pattern essentially restricts capabilities of analytical modeling. On the other hand, numerical solutions allow to obtain qualitative and quantitative evaluations of the process under study and to explain physical consequences. At the same time, mesh algorithms used in computer codes come across specific obstacles, which do not allow to calculate accurately wave fronts and high-gradient components localized at the loading area or propagated with time. One of such obstacles is the spurious effect caused by the mesh dispersion (*MD*) and responsible for the emergence of high-frequency "parasite" oscillations damaged the computer solution. This phenomenon manifested notably in the problems with singularities and multiple reflections, possessing own high-frequency patterns which are typical for compound structures and composites.

The present work is the further development of the so-called Mesh Dispersion Minimization (*MDM*) procedure in the finite difference method originally presented for *1D* wave processes in [1].

The studies of the *MD* in initial-boundary hyperbolical problems have a long-standing history and extensive literature: see, e.g., classical works [2,3] and some approaches to *MD* prevention presented in [4-7]. The algorithms minimizing *MD* have been also developed (see, e.g., [8-21]) for a wide spectrum of diverse mechanical, physical, geological-geophysical and other problems including even financial and stock exchange processes [22] where the issue of artificial oscillations separation from jump-wise solutions is of clear practical importance. Note that despite certain achievements in the analysis of spurious mesh effects and methods of their suppression, elimination or minimization of the *ND* remains topical (especially in case

of simulation of shock-pulse processes in inhomogeneous media and composite structures). There are a set of methods elaborated in this direction. For example, in work [9], where diffraction was explored of the plane elastic wave on the cylindrical cavity, the expansion in Fourier series along the circumferential coordinate was applied, and after that the problem was reduced to the *MDM* solution of a system of *1D* non-interconnected wave equations (each for its own harmonic). Then the sum of harmonics represents the final result. In [15], *MDM* algorithms were designed to solving a contact-impact elasticity problem. Following work [21], we have repeated that the *MDM* technique is based on a generalized concept of the Courant condition linked temporal and spatial mesh steps with the wave velocity, which reflects properties of the material at hand. The difference presentation of original differential equations exhibits some typical domains of dependence (*DD*), and the idea behind *MDM* is to properly adjust these *DD*s so as to improve convergence. This requirement allowed eliminating or minimizing *MD*. With this aim, phase velocities of high-frequency components of the continuous models have to be considered, and the mesh has to be design so that the propagation velocities induced by it approximate the former as closely as possible.

An important technical advantage of *MDM* is that it utilizes the same mesh for both high-gradient and smoothed components of the solution. The *MDM* principle was formulated in [1] as a requirement of coinciding dispersions in the continual and difference models. Following to this work, we show main points of *MDM* algorithms with the example of the classical wave equation (Section 2 in the present work) for the dispersionless waveguide (its simple analog in solid mechanics is a straight elastic rod). In this case, as shown in [1], it is possible to achieve a complete coincidence of *DDs*. The difference algorithm proves to be stable at the Courant number $\lambda = c_0\Delta t/\Delta x = 1$, where Δt and Δx are the dimensions of the difference grid in time and spatial coordinates correspondingly, c_0 is the sound velocity. The equality $\lambda = 1$ has the simple physical sense: during one step in time, the wave passes one spatial step. Here the solutions of continual and difference problems coincide in mesh points. In more complicated cases (Sections 3 – 5) *MDM* is attained by introducing special spatial approximation of functions and their derivatives. Such algorithms allow to obtain a solution, which is equally exact for both discontinuous solutions on a homogeneous grid. Note that implicit schemes having an infinite *DD* are inapplicable for describing discontinuous solutions.

2. HOMOGEMEOUS DISPERSIONLESS WAVEGUIDE

Consider the wave propagation problem in a semi-infinite dispersionless waveguide ($x \ge 0$) subjected by force F at free end $x = 0$. With use conventional designations, this classical one-dimensional problem has been formulated as follow:

$$u = u(x,t); \quad \ddot{u} = c_0^2 u'', \quad u'(0,t) = -F(t), \quad u(x,0) = \dot{u}(x,0) = 0, \qquad (1)$$

where u is displacement, c_0 is the sound speed, while parameters of the waveguide serves as measurement unites. Besides, zero initial conditions are added.

We begin with a steady-state solution for free wave propagation in the infinite rod ($|x| < \infty$). For the wave equation

$$\ddot{u} - c_0^2 u'' = 0, \qquad (1^*)$$

we will seek the steady-state solution using the Fourier form

$$u = U\exp[iq(ct \pm x)], \qquad (2)$$

where $U \sim \text{const}$, i is the imaginary unit, q is the wave number (then $l = 2\pi/q$ is the wavelength), c is the phase velocity (then $\omega = qc$ is the frequency).

Substitution (2) in (1^*) leads to the so-called dispersion equation:

$$c = \pm c_0. \qquad (3)$$

It determines dispersion-free wave propagation: phase velocity c is independent of the wave number q (or, that is the same, on the wavelength l). The *DD* for Eq. (1^*) is determined by the characteristic inequality $|x| \le c_0 t$.

A finite-difference analog of Eq. (1^*) with use in the explicit grid stencil of "cross" type is written as follows:

$$u_i^{k+1} = 2u_i^k - u_i^{k-1} + \lambda^2(u_{i+1}^k - 2u_i^k + u_{i-1}^k), \quad \lambda = c_0\Delta t/\Delta x, \qquad (4)$$

where $x = i\Delta x$; $t = k\Delta t$; i and k are coordinates of the current node of the mesh ($i = 0, \pm 1, \pm 2, \text{K}$, $k = 0, 1, 2, \text{K}$); λ is the Courant number. The stability condition of the algorithm (4) is $\lambda \le 1$ – the so-called *CFL* (Courant, Friedrichs, Lewy) condition.

Equation (4) is, generally speaking, dispersive. We have the following *DD* of (4): $|x| \le \lambda c_0 t$. Substituting a discrete analog of the solution (2),

$$u_i^k = U\exp[iq(ck\Delta t \pm i\Delta x)], \qquad (2^*)$$

into Eq. (4) we obtain the dispersion relation of the finite difference model,

$$c = \frac{2}{q\Delta t}\arcsin\left(\lambda \cdot \sin\frac{q\Delta x}{2}\right), \qquad (5)$$

which determines dependence of the phase velocity on the wavelength and mesh steps, Δx and Δt. The dispersion equation (5) has infinity of solutions (modes) that relate to multivalent *arcsine*. For sufficiently long waves ($l \to \infty \Rightarrow q \to 0$), the phase velocity corresponds to that in the continual problem: $c = c_0$. Difference in velocities (3) and (5) grows with decreasing wavelength and reaches its maximum at $l = 2\Delta x$ ($q = \pi/\Delta x = 2\pi/\lambda$ – is the minimal wavelength admissible for a discrete model). If $\lambda = c_0\Delta t/\Delta x = 1$ ($\Delta x = c_0\Delta t$ – during one time step, a wave with the velocity c_0 passes one spatial step), the *DDs* of two considered models coincide. As a result of this condition, the dispersion relation (5) passes into (3), and *MD* is completely eliminated.

Let us compare dispersive properties of both models. We assume Δx and c_0 as measurement units (then $\lambda = \Delta t$). Calculated from (5) dispersion curves $\omega(q) = cq$ for different values of λ are depicted in Fig. 1 (two modes are shown). If $\lambda \to 1$, these curves tend to the straight line $\omega = q$ (or $c = 1$ in the plain c,q) that determines the absence of dispersion. If $\lambda < 1$, phase velocities, $c = \omega/q$, of short waves decrease with q increasing in interval $(0, \pi)$, the wave process consists of long waves running ahead and short waves reaching the same point of the waveguide later than long those. If $\lambda > 1$, *DD* of the difference equation (4) becomes smaller than *DD* of equation (1), and the algorithm (4) loses stability. In a general case, we have no a closed analytical solution of the problem (4) but such a solution can be proved assuming $\lambda = 1$. By way

of example, we then examine impact loadings on the end of a semi-infinite waveguide $x \geq 0$ (1). Consider two types of boundary loading,

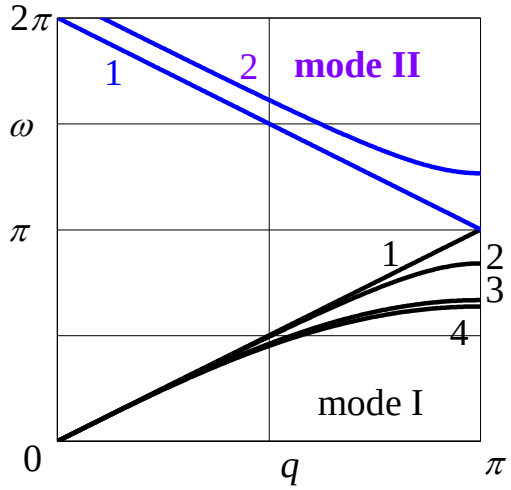

Fig. 1: Dispersion pattern in cases λ = 1 (curve 1), 0.95 (2), 0.9 (3) and 0.5 (4)

(*a*) the Heaviside step force $F(t) = -H(t)$, and

(*b*) the Dirac pulse $F(t) = -\delta(t)$.

In the case of the same finite difference problem, consider Eq. (4) with the corresponding boundary conditions at the so-called non-contour node numbered $i = -1$:

$$(a)\ u'(0,t) = -H(t) \Rightarrow u_{-1}^k = u_1^k + \Delta x\ (k \geq 0),$$

$$(b)\ u'(0,t) = -\delta(t) \Rightarrow,\ u_{-1}^0 = u_0^0 + \Delta x\ (k = 0),\ u_{-1}^k = u_0^k\ (k > 0). \qquad (6)$$

and zero initial conditions. In the continuous model, the well known d'Alambert solutions to these problems are

$$(a)\ u'(x,t) = -H(t-x),\quad (b)\ u'(x,t) = -1(x = t),\ u'(x,t) = 0\ (x \neq t). \qquad (7)$$

Remind that forces, stresses and strains are the same values due to the accepted measurement units.

In case $\lambda = 1$, equation (4) and boundary conditions are written as follows (here and below Δx = 1 is taken):

$$u_i^{k+1} = u_{i+1}^k + u_{i-1}^k - u_i^{k-1};\ (a)\ u_{-1}^k = u_0^k + 1,\ (b)\ u_{-1}^0 = u_0^0 + 1,\ u_{-1}^k = u_0^k\ (k > 0). \qquad (8)$$

By the mathematical induction technique, the following closed analytical solution of the problem (8) has been obtained for two versions of the loading (there is assumed: $\Delta x = \Delta t = c_0 = 1$):

$$(a)\ u'(x,t) = -H(k-i),\ (b)\ u'(x,t) = -1(k = i),\ u'(x,t) = 0\ (k \neq i), \qquad (9)$$

which coincide with analytical solutions (7) in mesh nodes.

For the two mentioned loadings, calculated distributions of strain $u'(x,t)$ along the *x*-axis at the moment of time t = 100 are shown in Fig. 2. Bold lines are analytical solutions and coincided with them numerical solutions for $\lambda = 1$, oscillating curves correspond to numerical solutions for $\lambda = 0.1$ and $\lambda = 0.5$.

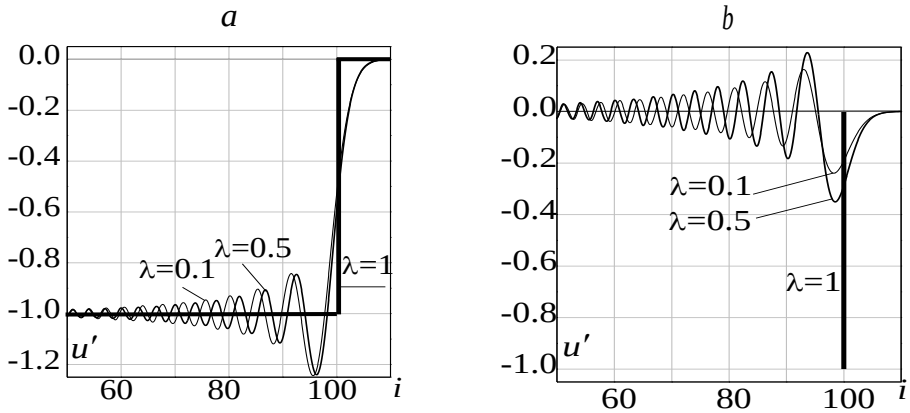

Fig. 2: Snapshots of strains at t = 100 for two kinds of loadings: (*a*) – the Heaviside step and (*b*)– the Dirac pulse. Bold lines are analytical solutions coincided with numerical solutions at λ = 1, oscillating curves are numerical solutions at different values of λ.

If $\lambda < 1$, the spurious effect of dispersion is essential in case (*a*), while the two solutions have nothing in common in case (*b*). We have the asymptotic solution of the problem (8) corrected at small λ and large i (or k) [23]. In case (*a*), it is the following:

$$u'(x,t) \sim -\left[\frac{1}{3} - \int_0^{\eta} Ai(z)dz\right],\ \eta = \frac{2(k\Delta t - i)}{(k\Delta t/3)^{1/3}},\ \mathrm{Ai}(z) = \frac{1}{\pi}\int_0^{\infty} \cos\left(zy + y^3\right)dy, \qquad (10)$$

where Ai(z) is Airy function. The form (10) is the general one for any dispersion waveguide loaded by the Heaviside step and determines the wave process in which a smoothed quasi-front propagates instead of the front, while high-frequency oscillations move behind it and fade with time. Asymptote (10) shows that the wave package spreads with time as $t^{1/3}$, the maximal amplitude of the wave remains constant and equals ~ −1.275. In Fig. 2 (*a*) calculated strains at λ < 1 practically coincide with the asymptote.

In the considered *1D* problem here and below, *MD* is completely eliminated from the numerical solution: the recent can be defined as "***the accurate numerical solution***" in the mesh nodes.

Note that *MD* elimination is impossible in implicit algorithms where the *DD* equals to infinity regardless of the size of mesh steps.

3. WAVEGUIDE UPON ELASTIC FOUNDATION

Consider the wave equation

$$\ddot{u} - c_0^2 u'' + G(u) = 0 \qquad (11)$$

(usually known as Klein-Gordon equation), where $G(u)$ is positive finite function.

3.1 Linear homogeneous foundation: $G(u) \equiv gu,\ g:\ const$.

Here Eq. (10) is written in the form

$$\ddot{u} - c_0^2 u'' + gu = 0. \qquad (11^*)$$

where g is the normalized rigidity of an elastic foundation (the measure units are the same as for the free waveguide above). Substituting the representation (2) into (11*), we obtain the following dispersion equation

$$c(q) = \sqrt{1 + g / q^2} \qquad (12)$$

In contrast with Eq. (1^*) for a free waveguide, Eq. (11^*) possesses wave dispersion. The *DD* of Eq. (11) is the same that in the previous case: $|x| \le c_0 t$. The explicit "cross"-type algorithm of the finite-difference analog of Eq. (11^*) has the form

$$u_i^{k+1} = 2u_i^k - u_i^{k-1} + \lambda^2 (u_{i+1}^k - 2u_i^k + u_{i-1}^k) + (\Delta t)^2 g u_i^k \quad (\lambda = \Delta t / \Delta x), \qquad (13)$$

where the notations of the previous problem are used. As above, Δx and c_0 are taken as measurement units: $\Delta x = c_0 = 1$, $\lambda = \Delta t$. The dispersion relation for Eq. (13) is

$$c = \pm \frac{2}{q \Delta t} \arcsin\left(\Delta t \sqrt{\sin^2 \frac{q}{2} + \frac{g}{4}} \right), \qquad (14)$$

that determines the following stability condition of the algorithm (13):

$$\Delta t \le 1 / \sqrt{1 + g/4}. \qquad (15)$$

It is turned out that *DD* of Eq. (13) is $|x| \le t\sqrt{1 + g/4}$ that always exceeds *DD* of the continual problem: ($|x| \le t$). So, the appeared *MD* inevitably distorted the solution.

Our aim is to construct for the discrete analog of (11) such a difference scheme that the dispersion relation of which is maximally closes to (12). One can overcome this obstacle using a special difference approximation of Eq. (11) introduced in [1]: instead of the ordinary local presentation $gu \sim gu_i^k$ in Eq. (13), the non-local average form is used as the following three-point approximation:

$$gu \sim g(u_{i+1}^k + 2u_i^k + u_{i-1}^k)/4. \qquad (16)$$

In this case, the conventional algorithm (13) is written as the following:

$$u_i^{k+1} = 2u_i^k - u_i^{k-1} + \lambda^2 [(u_{i+1}^k - 2u_i^k + u_{i-1}^k) + g(u_{i+1}^k + 2u_i^k + u_{i-1}^k)/4]. \qquad (17)$$

It can be readily shown that the approximation orders of Eqs. (13) and (17) are the same: $(\Delta t)^2 + (\Delta x)^2$. For Eq. (17), the dispersion relation acquires the following form:

$$c = \pm \frac{2}{q \Delta t} \arcsin\left(\Delta t \sqrt{\sin^2 \frac{q}{2} + \frac{g}{4} \cos^2 \frac{q}{2}} \right). \qquad (18)$$

If we set $\lambda = 1$ in (18) and examine extremely short waves of length $l = 2$, whose propagation velocity determines *DD* of the difference problem, it turns out that *DD* coincide ($|x| \le t$) for both differential and difference problems, while the stability condition corresponds to the *CFL*-criterion $\lambda \le 1$ as in the previous case $g = 0$. Thus, waves of minimal length ($l = 2$) propagate at the same velocity $c = 1$ as infinitely short waves [$l \to 0 \quad (q \to \infty)$] in the continual model. As in the free waveguide above, *MD* is completely eliminated over the entire discrete spectrum.

Let us compare the computation results related to the transient problem. We have added zero initial conditions to equations (17), and the boundary condition in the case of a semi-infinite system ($x \ge 0$). We have used the boundary condition as action of the step-wise stress at the end $x = 0$: $\sigma(0,t) = -\sigma_0 H(t - t_0)$, where σ_0 and t_0 are the pulse amplitude and duration.

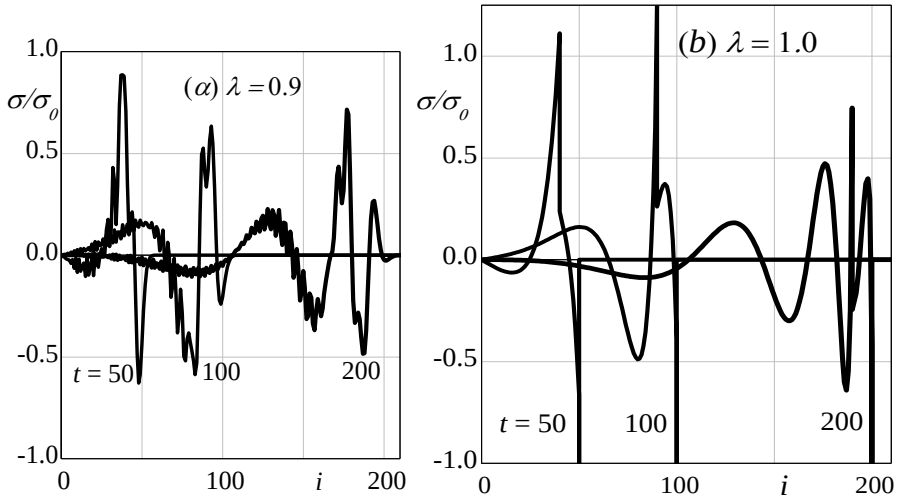

Fig. 3: Comparison of computer solutions for normalized stress propagated along the rod with elastic foundation of the rigidity g = 0.01 under action of pulse with duration t_0 = 10.In the left picture, calculation results corresponds to conventional algorithm (13) with λ = 0.9, while the *MDM* algorithm (17) with λ = 1.0 leads to results depicted in the right.

The comparison of results presented in Fig. 3 shows the essential distortion of the solution obtained by the conventional algorithm (13), while calculations with the *MDM* algorithm (17) can be considered as exact one in mesh nodes: spurious oscillations are absent, and front gaps are clearly detected.

Calculation results presented below are obtained with *MDM* algorithms.

3.2 Linear inhomogeneous foundation

Note that the introduced above three-point approximation (16) within *MDM*-algorithms used also in the case of the inhomogeneous foundation: $g \equiv g(x)$. Although the dispersion equation is absent here, the use of the so-called method of frozen coefficients can be leaded to the goal: we denote $g = \max_x |g(x)|$ and change variables in (13): $\bar{x} = x\sqrt{g}$, $\bar{t} = t\sqrt{g}$. After that *MDM* algorithm (17) is launched.

3.3 Nonlinear foundation

Consider wave propagation processes in a semi-infinite thin rod ($x \geq 0$) leaned upon a nonlinear foundation. Let boundary and initial conditions be the same that were used above. Then the considered initial-boundary problem is formulated as follows:

$$\ddot{u} - c_0^2 u'' + G(u)u = 0,\ \varepsilon(0,t) = u'(0,t) = -F(t)\ ,\ u(x,0) = \dot{u}(x,0) = 0,$$

$$\varepsilon(0,t) = u'(0,t) = -F(t)\ ,\ u(x,0) = \dot{u}(x,0) = 0, \qquad (19)$$

where $u \equiv u(x,t)$, $G(u)$ is finite positive odd (with respect to u) function.

Let (without loss of generality), function $G(u)$ has the following kind:

$$G(u) = gu\left[1 + g_0 u^2\right],$$

which is chosen as the beginning of the Taylor expansion of odd function $G(u)$.

If $g_0 = 0$, we have the linear case considered above.

Our aim is to design the *MDM* algorithm to calculate the problem (19) and by the computer simulation to reveal the influence of nonlinearity on the wave propagation process. Completed tests show that the *MDM* representation

$$G(u) \Rightarrow gU\left(1+g_0U^2\right), \quad U=\frac{u_{j+1}^k+2u_j^k+u_{j-1}^k}{4} \tag{20}$$

together with condition λ =1 result in the dispersionless algorithm

$$u_i^{k+1}=u_{i+1}^k+u_{i-1}^k-u_i^{k-1}+gU\left(1+g_0U^2\right),$$

allowing linear and nonlinear problems to be calculated on the same mesh and by the same accuracy. In Fig. 4 (*a*,*b*), snapshots of linear and nonlinear wave patterns of strains are compared at t =250. Fig. 4 (*b*) shows the same results in an extended scale along the x axis near the wave front. The related results show that the fundamental difference in front zone is not found in linear and nonlinear solutions (despite of the relatively huge value of g_0). This surprising (at first sight) result can be explained by the fact that the package of high frequency oscillations generating in the front zone, propagates together with the front, while the perturbations related to the presence of the foundation (and, in this way, the nonlinearity) moves behind the front zone.

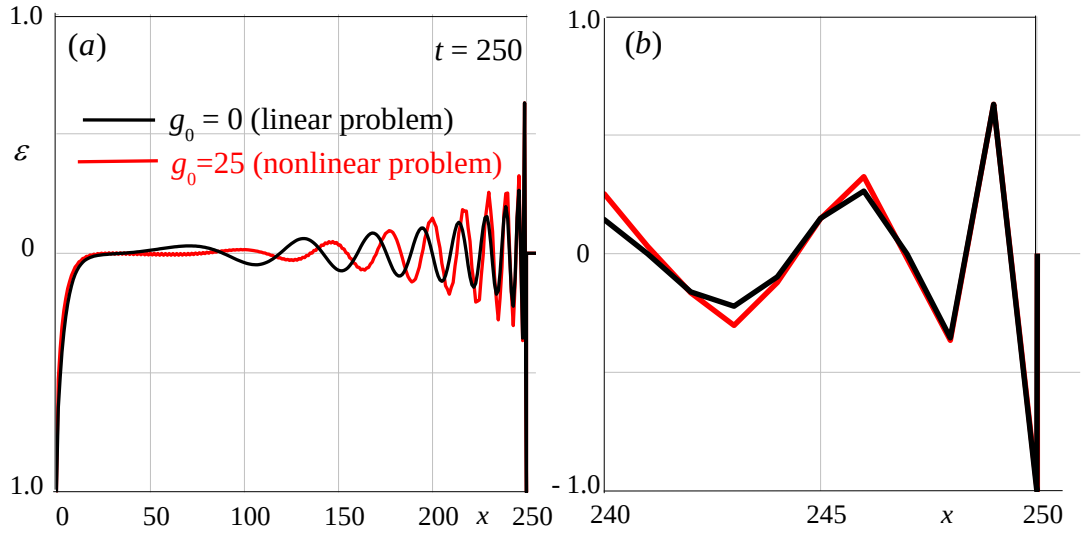

Fig. 4: Snapshots of the strain distributions in linear and nonlinear problems ($\Delta x=\Delta t=1,\ c_0=1,\ g=0.05,\ g_0=25$).

4. SPHERICAL AND CYLINDRICAL WAVES

Consider the following wave equation possessing the inhomogeneous term:

$$\ddot{u}=c_0^2u''+B(x)u', \tag{21}$$

($B(x)$ is the finite function) which can describe various models of continual media, for example, elastic waves in a thin rod of the variable the cross-section area or cylindrical and spherical waves in a compressible liquid under action of linear or point sources, respectively.

In general, Eq. (21) does not have a dispersion equation. As above, in Section 2, we apply the frozen coefficients method (assume $|B(x)| \le \overline{B} \sim$ const) and the standard Fourier analysis to the difference analog of equation (21):

$$u_i^{k+1} - 2u_i^k + u_i^{k-1} = \lambda^2(u_{i+1}^k - 2u_i^k + u_{i-1}^k) + \lambda\,\Delta t\,\bar{B}(u_{i+1}^k - u_{i-1}^k)/2,\ \lambda = \Delta t/\Delta x. \quad (22)$$

Then the resulting dispersion equation

$$c(q,\Delta x,\Delta t) = \frac{2}{q\Delta t}\arcsin\left[\lambda\sqrt{\sin^2\frac{q\Delta x}{2} + \frac{\bar{B}\Delta x}{4\lambda}\sin(q\Delta x)}\right]$$

(23)

shows that in case of $\lambda = 1$, maximally short waves $(q\Delta x = \pi)$ have the phase velocity c =1 as in the homogeneous case. Then the *MDM* algorithm for calculation of the equation (22) with use equality $\lambda = 1$ is proved as follows:

$$u_i^{k+1} = u_{i+1}^k + u_{i-1}^k - u_i^{k-1} + \Delta t\,B\left(i\Delta x\right)(u_{i+1}^k - u_{i-1}^k)/2.$$

(24)

Let consider spherical (*a*) and cylindrical (*b*) waves in a compressible liquid. We set $B(x) = \alpha/x$ then Eq. (24) is rewritten as

$$\ddot{u} = u'' + (\alpha/x)u',\ \ x \ge 0, \quad (25)$$

which describes cylindrical $(\alpha = 1)$ or spherical $(\alpha = 2)$ pressure waves. Here u plays role of the velocity potential in the compressible liquid, x – radial coordinate. Radial velocity and pressure of the wave are expressed respectively as $\dot{u} = \partial u/\partial x$ and $P = -\partial u/\partial t$ (the bulk compression modulus and the liquid density serve as measurement units). Under the condition $\lambda = 1$, the Eq. (25) is calculated by the following *MDM* algorithm $(\Delta x = \Delta t = 1)$:

$$u_i^{k+1} = u_{i+1}^k - u_i^{k-1} + u_{i-1}^k + \frac{\alpha}{2(x_0 + i\Delta x)}(u_{i+1}^k - u_{i-1}^k), \quad (26)$$

where x_0 is the source radius.

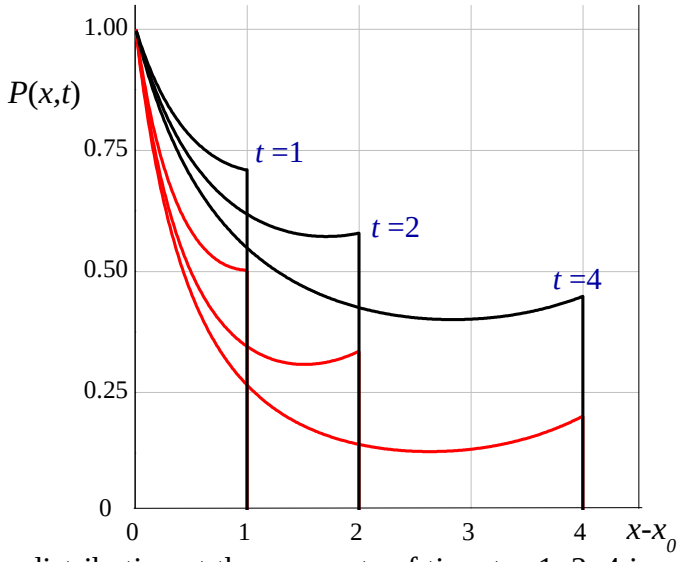

Fig. 5: Pressure distribution at the moments of time t = 1, 2, 4 in spherical (red lines) and cylindrical (black lines) waves under action of pressure $P(1,t) = H(t)$ on cavity surface $x = 1$.

Pressure of the Heaviside type is set on cavity surfaces in the both cases:

$$x_0 = 1:\ P(1,t) = H(t)$$

Calculated by *MDM* algorithm (26) snapshots of the pressure distributions along the radial coordinate at time values t = 1, 2 and 4 are shown in Fig. 5. The

obtained numerical solutions completely agree with analytical ones (see, e.g., [23]). Note that an analytical solution for the cylindrical case is available only in the vicinity of the front. Calculations show that application of conventional difference algorithms with $\lambda < 1$ leads, as in the previous cases to a significant distortion of the solution.

5. WAVES IN COMPOSITE STRUCTURES

Consider *MDM*-algorithms and calculation results related to the pulse propagation process in semi-infinite composite structures $(x \geq 0)$ subjected by the action of the Heaviside step applied in the free end $(x = 0)$ of the each system.

5.1 Rods with a periodic system of rigidly connected inertial particles

The mathematical formulation of the problem is as follows:

$$M\ddot{u} = c_0^2 u'', \quad M = 1 \ (x = n + X,\ 0 < X < L), \quad M = m \ (x = n), \quad n = 0,1,2,\text{K}$$
$$u'(0,t) = H(t), \quad u(x,0) = 0, \quad \dot{u}(x,0) = 0, \tag{27}$$

where L is the distance between particles (period), m is the mass of the adjoined particle. The Young modulus of the rod material, E, its density, ρ, and L are measurement units: $E = \rho = L = 1$, $(c_0 = \sqrt{E/\rho} = 1)$. The *MDM* algorithm with $(\Delta x = \Delta t = 1)$ for the difference analog of (27) is built similarly to that in the homogeneous case (8):

$$Mu_i^{k+1} = 2(M-1)u_i^k + u_{i+1}^k + u_{i-1}^k - Mu_i^{k-1};\ u_{-1}^k = u_0^k + 1, \quad u_{-1}^0 = u_0^0 = 0. \tag{28}$$

The main physical feature of the considered system is the following: for propagation of short waves (forming the front zone), particles of finite mass are insuperable obstacles – after incoming the Heaviside front, inertial medium immediately deviate it into a quasi-front, which spreads with along wave propagation from the source. Strains $\varepsilon = \partial u/\partial x$ vs. time calculated in cross-section x = 40 are shown in Fig. 6 (*a*) (m = 3). Computer results are practically not differing from the long-wave asymptote of type (10). With the taken parameter m = 3, the quasi-front velocity is $C_* = 1/\sqrt{1+m} = 0.5$. This is the reason, why the wave process in the cross-section x = 40 begins to be developed ~ at $t \geq 80$.

5.2 Periodic system of rods serially connected by inertionless springs

As in the previous case, parameters of an elementary rod are measurement units: $E = \rho = L = 1$, but instead of the mass parameter m, the spring rigidity, g, is introduced here. Without dwelling on the mathematical formulation of the problem, let us say that the *MDM* algorithm is built with the condition $\Delta x = \Delta t = 1$, that allows to obtain calculation results without *ND*.

The stability condition is $g \leq g^*$ $(g^* = ES/\Delta x)$ where g^* is the rigidity of the rod with the length equal to Δx (S is the cross-section square of the rod).

The curve in Fig. 6 (*b*) (g = 0.1, L = 10) show the strain vs. time in cross-section x = 105 (the median of the 11th rod element in the system). As in the previous case, practically complete coincidence with the asymptotical form (10) is detected, and the

main dynamic overhead traveling within the quasi-front zone is precisely described by

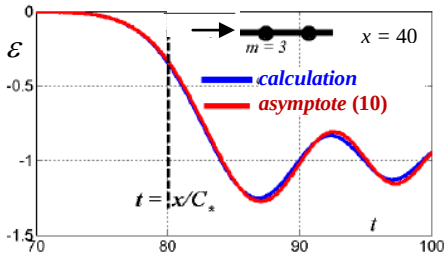

(*a*) Rod with massive particles (m = 3)

Fig. 6: Waves in composite structures subjected by the Heaviside loading $u'(0,t) = -H(t)$

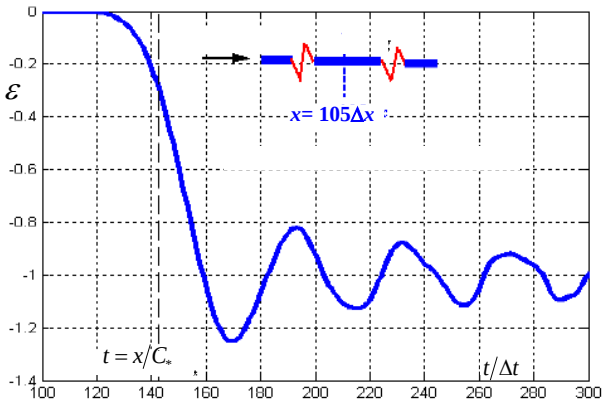

(*b*) Rods connected by inertionless springs

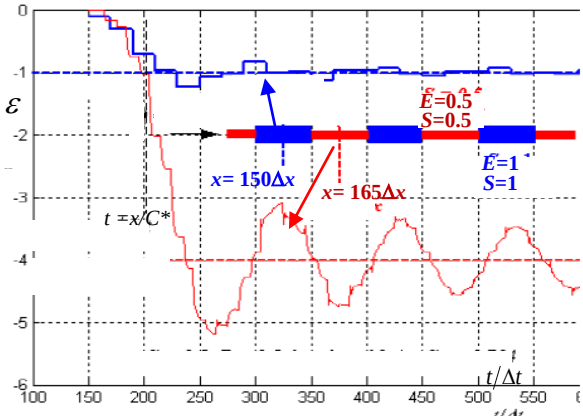

(*c*) Double-periodic rod system

5.3 Double-periodic system of serially connected rods

This model is transformed from model 5.2 if a material spring of the given length (rod) is used instead of the spring. The length of the composite unit (period) is taken as length unit (L = 1), it consists of two elementary rods 1 and 2 of lengths l and $1 - l$ correspondingly. In addition to parameters of rods used above we introduce parameters of cross-section squares, S_1 and S_2. From the continual formulation of the problem including equations of motion of internal points:

$$\text{rod 1: } \ddot{u}_{1,n} = c_1^2 u''_{1,n} = 0 \quad (0 \le X \le l), \quad (n = 0, \pm 1, \pm 2, \text{K}),$$
$$\text{rod 2: } \ddot{u}_{2,n} = c_2^2 u''_{2,n} \quad (l \le X \le 1); \quad x = n + X, \tag{29}$$

boundary conditions at the connection points:

$$\begin{aligned} X = 0&: \quad u_{1,n} = u_{2,n-1}, \quad E_1 S_1 u'_{1,n} = E_2 S_2 u'_{2,n-1}; \\ X = l&: \quad u_{1,n} = u_{2,n}, \quad E_1 S_1 u'_{1,n} = E_2 S_2 u'_{2,n}; \\ X = 1&: \quad u_{2,n} = u_{1,n+1}, \quad E_1 S_1 u'_{1,n+1} = E_2 S_2 u'_{2,n}, \end{aligned} \tag{30}$$

and boundary and zero initial conditions

$$\varepsilon_0 = u'(0,t) = -H(t), \; u(x,0) = \dot{u}(x,0) = 0,$$

the following MDM algorithm is built provided the accurate computer solution:

1. Motion of internal nodes inside the period:

$$u_{1,j}^{k+1} = u_{1,j+1}^{k} + u_{1,j-1}^{k} - u_{1,j}^{k-1},\ j \in \left(0, J_1 = l/\Delta x_1\right)$$
$$u_{2,j}^{k+1} = u_{2,j+1}^{k} + u_{2,j-1}^{k} - u_{2,j}^{k-1},\ j \in \left(0, J_2 = (1-l)/\Delta x_2\right) \quad (31)$$

2. Equations for nodes connecting rods:

$$x = n,\ X = 0 \Rightarrow U_n^{k+1} = 0.5[u_{1,1}^{k}(1+\gamma) + u_{2,J_2-1}^{k}(1-\gamma)] - U_n^{k-1},$$
$$x = n,\ X = l \Rightarrow\ V_n^{k+1} = 0.5[u_{1,J_2-1}^{k}(1-\gamma) + u_{2,1}^{k}(1+\gamma)] - V_n^{k-1}, \quad (32)$$
$$\gamma = S_1\rho_1\Delta x_1 + S_2\rho_2\Delta x_2,\ U_n^{k} = \left(u_{1,0}^{k}\right)_n = \left(u_{2,J_2}^{k}\right)_n,\ V_n^{k} = \left(u_{1,J_1}^{k}\right)_n = \left(u_{2,0}^{k}\right)_n.$$

3. *MDM* relations: $\Delta x_s = c_s\Delta t\ (s = 1,2)$. (33)

4. Boundary and zero initial conditions:

$$u_{1,-1}^{k} = u_{1,0}^{k} + 1,\ [u]_i^{-1} = [u]_i^{0} = 0,\ [u] = u_1, u_2. \quad (34)$$

In the example of calculation of system (31)–(34) presented in Fig. 6(*c*), strains are depicted vs. time in the two marked cross-sections of the system. As in two previous cases, the asymptote (10) sufficiently reproduces calculation data (excluding disturbances related to multiple reflections from nodes). The difference of average strains in two different rods in the period corresponds to the static relation of the forces equality: $E_1S_1\varepsilon_1 = E_2S_2\varepsilon_2$.

5.4 Unidirectional reinforced composite loaded along the fiber direction

A plane problem for waves propagated in the composite shield is considered. The shield occupies half-plane $x \geq 0$ and consists of a regular system alternating extensible fibers (black thick lines in the scheme inserted in Fig .7) and pliable layers of the adhesive (shaded).

There is assumed in the mechanical model that fibers function in tension-compression, while the adhesive is under shear stress (only one-directional longitudinal displacements propagate in the shield). The assumption that normal stresses exist only in fibers and tangential stresses – only in the adhesive is often used in studying static equilibrium of unidirectional composites. Such structures have wide range of practical application (for example, in aircraft and ship engineering). Although the stress state of structure components is, in fact, more complex, such approach correctly expresses the main concept of the efficient performance of a reinforced material: high strength fibers are oriented along the tensile stress lines, while the adhesive facilitates a more uniform distribution of these loads between fibers, preventing stress concentrations.

We use the following notations: *h*, *E*, and ρ_f are correspondingly the fiber width, Young modulus of the fiber material and its density; the adhesive has width *H*, shear modulus *G*, and density ρ_a. Axis *x* is directed along the fibers, and axis *y* – across them. Then assume *h* << *H* and introduce local coordinate *Y* varied inside interval $0 < Y < H$, then $y = nH + Y$, $(n = 0 \pm 1, \pm 2, \text{K})$. Displacements and stresses in fibers are denoted by $u_n(x,t)$ and $\sigma_n(x,t)$, in adhesive – $v_n(x,Y,t)$ and $\tau_n(x,Y,t)$.

The motion of fibers is described by the system of wave equations for rods with the action of the shear stresses in contact lines:

$$\begin{aligned} &\rho_f h \ddot{u}_n = Eh(u_n)''_{xx} + \tau_n^+(x) - \tau_n^-(x), \quad n = 0, \pm 1, \pm 2, \text{K} \\ &\tau_n^+ = G(v_n)'_Y\Big|_{Y=0}, \quad \tau_n^- = G(v_{n-1})'_Y\Big|_{Y=H} \end{aligned}, \tag{35}$$

while motion of the adhesive is described by the system of 2D wave equations:

$$0 \le Y \le H: \quad \ddot{v}_n = c_a^2 (v_n)''_{YY} \quad \left(c_a = \sqrt{G/\rho_a}\right). \tag{36}$$

The zero initial conditions are postulated:

$$u_n(x,0) = v_n(x,y,0) = 0, \quad n = 0 \pm 1, \pm 2, \text{K} \tag{37}$$

Finally, conditions of the rigid connection of fibers and adhesive are:

$$v_n(x,0,t) = u_n(x,t), \quad v_n(x,H,t) = u_{n+1}(y,t) \tag{38}$$

Remind that this work is aimed to building the *MDM* algorithm for calculation of wave pattern in such a composite and the detail analysis of its dynamic features of interest can be associated say in process. With this reason, the simplified case of loading is chosen: all fibers simultaneously subjected by Heaviside axial stress σ_0 at the line *x* = 0:

$$\sigma_n(0,t) = H(t). \tag{39}$$

Then, due to the obvious periodicity of the problem with respect to axis *y*, only one fiber (let it be *n* = 0) and the half of the adhesive layer ($0 < y < H/2$) can be considered. Then the system (35) is transformed in the only equation:

$$\rho_f h \ddot{u} = Eh u''_{xx} + 2G v'_y\Big|_{y=0}, \tag{40}$$

Eq. (36) is remained here:

$$0 \le y \le H/2: \quad \ddot{v}_n = c_a^2 v''_{yy} \tag{41}$$

and the boundary conditions for the adhesive have the following form:

$$v(x,0,t) = u(x,t), \quad \tau(x,H/2,t) = G v'_y(x,H/2,t) = 0 \tag{42}$$

Omitting intermediate considerations, we present the *MDM* algorithm for precise numerical solution of the problem (39) – (42):

fiber: $u_i^{k+1} = u_{i+1}^k + u_{i-1}^k - u_i^{k-1} + 2g v_{i,1}^k;$

adhesive: $v_{i,j}^{k+1} = v_{i,j+1}^k + v_{i,j-1}^k - v_{i,j}^{k-1}, \quad j = 1, 2, ..., J, \; J = H/(2\Delta y);$

$$g = GH/\left(Ehm^*\right), \; m^* = h\rho_f \Delta x + H\rho_a \Delta y; \quad \Delta x = c_f \Delta t, \; \Delta y = c_a \Delta t; \tag{43}$$

boundary conditions: $v_{i,0}^k = u_i^k, \quad v_{i,J+1}^k = v_{i,J-1}^k;$

loading: $u_{-1}^k = u_1^k + \Delta x \sigma_0 / Eh,$ initial conditions: $u_i^0 = u_i^{-1} = v_{i,j}^0 = v_{i,j}^{-1} = 0$

An example of calculation of the system (43) is presented in Fig. 7 where stresses in three cross-sections of the fiber are shown vs. time. (parameters of the composite: H/h =4, G/E =0.25, ρ_f / ρ_a =1 (m^*=4, c_a = 0.5c_f, C_* = 0.5).

The main feature of the composite dynamics is the following: perturbations propagating in the fiber continuously excite transversal shear waves in the adhesive layer which, in their turn, reflected from fibers. The reflected and re-reflected waves are characterized by incoming of sharp peaks whose time of life and amplitude continuously decreased with time. In spite of the local variability of the wave pattern and appearance of discontinuities, the spread part of the wave moving along the fiber can sufficiently be described by longwave asymptote (10), which marked by the dashed curve in Fig. 7.

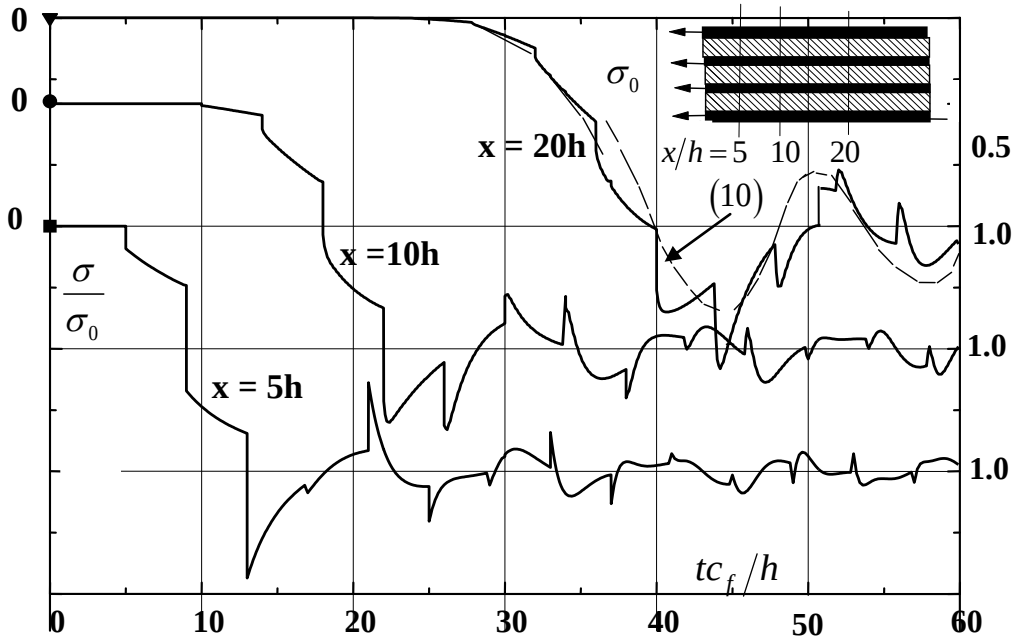

Fig 7: Axial stresses in fibers of the unidirectional composite shield vs. time**.**

REFERENCES

1. S.A. Abdukadirov, N.I. Pinchukova and M.V. Stepanenko, "A numerical approach to solving dynamic equations of elastic media and structures," J. Mining Sci., No. 6 (1984).
2. H.F. Weinberger, "Upper and lower bounds for eigenvalues by finite difference methods," Comm. Pure Appl. Math, Vol. 9 (1956).
3. P.D. Lax and B.Wendroff, "Difference schemes for hyperbolic equations with high order of accuracy", Comm. Pure Appl. Math., Vol. 17 (1964).

4. J.E. Fromm, "A method for reducing dispersion in convective difference schemes", J. Comput. Phys, 3, 2 (1968).
5. R.C.Y. Chin, "Dispersion and Gibbs phenomenon associated with difference approximations to initial boundary-value problems for hyperbolic equations", Journal of Calculational Physics, Vol. 18 (1975).
6. S.A. Abdukadirov and M.V. Stepanenko, “On elastic wave dispersion in continual and difference models of deformable media and structures”, in: "Numerical Methods of Problems Solvlng of Elasticity and Plasticity Theories [in Russian], Part 2, Ed. ITPM Sib. Branch. USSR Acad. Scie., Novosiblrsk (1980).
7. S. A. Abdukadirov, “Diffraction of non-steady-state plane elastic wave on a cylindrical cavity", In: Reports to Conf. ‘Propagation of Elastic and Elastic-Plastic Waves’ [in Russian], Frunze (1983)
8. A.I. Belov, V.A. Kornilo, N.I. Pinchukova and M.V. Stepanenko, "Reaction of a three-layer hydroelastic cylindrical shell on the effect of axisymmetric internal explosion," J. Appl. Mech. Tech. Phys., No. 1 (1986).
9. S.A. Abdukadirov, N.I. Alexandrova, M.V. Stepanenko, "Non-stationary diffraction of a plane longitudinal wave on an elastic cylindrical shell," Mechanics of Solids, No. 5 (1989).
10. S.A. Abdukadirov, K.K. Kurmanaliev and M.V. Stepanenko, "Dynamic stresses on the boundary of rigid inclusions embedded in rock massif," J. Mining Sci., 5 (1988).
11. A.L. Smirnov, "Calculation of the impact driving of piles into soil," J. Mining Sci., 4 (1989).
12. L. Slepyan, M. Ayzenberg-Stepanenko, "Superplastic Protective Structures," in: Progress in Industrial Mathematics at ECMI 96, Stuttgart. Teubner (1997).
13. L. Slepyan, M. Ayzenberg-Stepanenko, "Penetration of metal-fabric composite targets by small projectiles," in: Personal Armor Systems. British Crow Copyright/MOD, Colchester, UK (1998).
14. M.V. Ayzenberg-Stepanenko, L.I. Slepyan, "Localization of strain and melting wave in high-speed penetration", in: IUTAM Symp. on Nonlinear Singularities, Kluwer (1999).
15. V.D. Kubenko and M.V. Ayzenberg-Stepanenko, "Impact indentation of a rigid body into elastic layer. Analytical and numerical approaches," Journal of Math. Sciences, No. 1 (2009).
16. D. Gabriel, J. Plešek, R. Kolman and F. Valeš. Dispersion of elastic waves in the contact–impact problem of a long cylinder. Journal of Computational and Applied Mathematics, V. 234 (2010), 1930-1936
17. Z. Sun, Y. Ren, C. Larricq, S. Zhang, Y.Yang. A class of finite difference schemes with low dispersion and controllable dissipation for DNS of compressible turbulence. J. Comp. Physics, 2011, 230 (12), https://doi.org/10.1016/j.jcp.2011.02.038
18. Y.S. Wu, P.A. Forsyth, "Efficient schemes for reducing numerical dispersion in modeling multi-phase transport through heterogeneous geological media," Vadose Zone Journ., 7, No. 1 (2008).
19. M.V. Ayzenberg-Stepanenko, G.G. Osharovich, E.N. Sher, Z.Sh Yanovitskaya, "Numerical simulation of shock-wave processes in elastic media and structures. Part I: Solving method and algorithms", Journal of Mining Science 48, 1 (2012).
20. Y.Zhou, D.Yang, X. Ma and J.Li. An effective method to suppress numerical

dispersion in 2D acoustic and elastic modeling using a high-order Padé approximation. J.of Geophysics and Engineering, 2015, 12 (1).
21. Wu, Z. and Alkhalifah,T. A highly accurate finite-difference method with minimum dispersion error for solving the Helmholtz equation. J. Computational Physics**,** V. 365 (2018). https://doi.org/10.1016/j.jcp.2018.03.046
22. R. Int-Veen, "Avoiding numerical dispersion in option valuation," *Comp.Visual. Sci.*, Vol. 10, No. 4 (2007).
23. L.I.Slepyan. Non-steady-state elastic waves. Sudostrojenie. Leningrad 1972 (in Russian).